

Gene amplification of chromatin remodeling factor *SMARCC2* and low protein expression of *ACTL6A* are unfavorable factors in ovarian high-grade serous carcinoma

NAOMI MAGARIFUCHI^{1,2}, TAKESHI IWASAKI¹, YOSHIHIRO KATAYAMA^{1,2}, TAKUMI TOMONAGA¹, MIYA NAKASHIMA^{1,2}, FUMIYA NARUTOMI¹, KIYOKO KATO² and YOSHINAO ODA¹

Departments of ¹Anatomic Pathology and ²Gynecology and Obstetrics, Graduate School of Medical Sciences, Kyushu University, Fukuoka, Fukuoka 812-8582, Japan

Received October 4, 2023; Accepted January 23, 2024

DOI: 10.3892/ol.2024.14329

Abstract. Ovarian high-grade serous carcinoma (OHGSC) is the most common type of ovarian cancer worldwide. Genome sequencing has identified mutations in chromatin remodeling factors (CRFs) in gynecological cancer, such as clear cell carcinoma, endometrioid carcinoma and endometrial serous carcinoma. However, to the best of our knowledge, the association between CRFs and OHGSC remains unexplored. The present study aimed to investigate the clinicopathological and molecular characteristics of CRF dysfunction in OHGSC. CRF alterations were analyzed through numerous methods, including the analysis of public next-generation sequencing (NGS) data from 585 ovarian serous carcinoma cases from The Cancer Genome Atlas (TCGA), immunohistochemistry (IHC), and DNA copy number assays, which were performed

on 203 surgically resected OHGSC samples. In the public NGS dataset, the most frequent genetic alteration was actin-like protein 6A (*ACTL6A*) amplification at 19.5%. Switch/sucrose non-fermentable related, matrix associated, actin dependent regulator of chromatin subfamily c member 2 (*SMARCC2*) amplification (3.1%) was associated with significantly decreased overall survival (OS). In addition, chromodomain-helicase-DNA-binding protein 4 (*CHD4*) amplification (5.7%) exhibited unfavorable outcome trends, although not statistically significant. IHC revealed the protein expression loss of ARID1A (2.5%), SMARCA2 (2.5%) and SMARCA4 (3.9%). The protein expression levels of *ACTL6A*, *SMARCC2* and *CHD4* were evaluated using H-score. Patients with low protein expression levels of *ACTL6A* showed a significantly decreased OS. Copy number gain or gene amplification was demonstrated in *ACTL6A* (66.2%) and *SMARCC2* (33.5%), while shallow deletion or deep deletion was demonstrated in *CHD4* (70.7%). However, there was no statistically significant difference in protein levels of these CRFs, between the different copy number alterations (CNAs). Overall, OHGSC exhibited CNAs and protein loss, indicating possible gene alterations in CRFs. Moreover, there was a significant association between the protein expression levels of *ACTL6A* and poor prognosis. Based on these findings, it is suggested that CRFs could serve as prognostic markers for OHGSC.

Correspondence to: Professor Yoshinao Oda, Department of Anatomic Pathology, Graduate School of Medical Sciences, Kyushu University, 3-1-1 Maidashi, Higashi, Fukuoka, Fukuoka 812-8582, Japan
E-mail: oda.yoshinao.389@m.kyushu-u.ac.jp

Abbreviations: *ACTL6A*, actin-like protein 6A; ARID1A, AT-rich interaction domain 1A; ATP, adenosine triphosphate; CHD, chromodomain-helicase-DNA-binding protein; CNA, copy number alteration; CRF, chromatin remodeling factor; FFPE, formalin-fixed and paraffin-embedded; FIGO, International Federation of Gynecology and Obstetrics; H3K27me3, tri-methylation of lysine 27 of histone H3; IHC, immunohistochemistry; NGS, next-generation sequencing; OHGSC, ovarian high-grade serous carcinoma; OS, overall survival; PCR, polymerase chain reaction; SWI/SNF, switch/sucrose non-fermentable; SMARCA, SWI/SNF related, matrix associated, actin dependent regulator of chromatin subfamily a; SMARCB, SWI/SNF related, matrix associated, actin dependent regulator of chromatin subfamily b; SMARCC, SWI/SNF related, matrix associated, actin dependent regulator of chromatin subfamily c; TCGA, The Cancer Genome Atlas

Key words: CRF, OHGSC, CNA

Introduction

Ovarian high-grade serous carcinoma (OHGSC) is the most common type of epithelial ovarian cancer, accounting for 60% of all ovarian malignancies and 70% of ovarian cancer-related deaths in the United States (1,2). Survival in OHGSC is influenced by numerous factors, such as age, cancer stage and the size of residual tumor after cytoreductive surgery (3,4). Epigenetic dysregulation has been recognized as a significant factor in cancer development, progression and chemoresistance (5). These alterations involve abnormal DNA methylation patterns, disrupted histone posttranslational modifications, and changes in chromatin composition and/or organization (6). Chromatin remodeling factors (CRFs) serve a vital role in modifying chromatin structure, regulating the accessibility of DNA to

transcription factors and machinery and thereby dynamically influencing gene expression (7). Genome sequencing studies have revealed a high prevalence of CRF mutations across numerous cancer types (8). In the context of gynecological cancer, AT-rich interaction domain 1A (*ARID1A*) mutations have been identified in 35-46% of ovarian clear cell carcinoma, 30-63% of ovarian endometrioid carcinoma, 6% of endometrial serous carcinoma and 14% of carcinosarcoma cases (9-11). Chromodomain-helicase-DNA-binding protein 4 (*CHD4*) somatic mutations have been detected in 17% of endometrial serous carcinoma (10), while switch/sucrose non-fermentable (SWI/SNF) related, matrix associated, actin dependent regulator of chromatin (SMARCA) subfamily a member 4 (*SMARCA4*) germline and somatic mutations have been found in 69% of cases of small cell carcinoma of the ovary, hypercalcemic type (12). A previous study reported that *CHD4* mRNA expression is significantly higher in platinum-resistant cases compared with in platinum-sensitive cases of OHGSC and ovarian clear cell carcinoma (13). Despite these findings, to the best of our knowledge, there has not been a comprehensive and large-scale investigation exploring the association between CRFs and OHGSC.

In the present study, a comprehensive analysis of OHGSC cases from histological, immunohistochemical and genetic perspectives was conducted to elucidate the role of CRF dysfunction in OHGSC.

Materials and methods

Public data analysis. The cBioPortal (<http://www.cbioportal.org/>) (14,15) was used to retrieve public whole exome sequencing data and mRNA sequencing data for ovarian serous carcinoma. Initially, 'Ovary/Fallopian Tube' was selected in the 'Select Studies for Visualization & Analysis' and the Ovarian Serous Cystadenocarcinoma dataset [The Cancer Genome Atlas (TCGA), PanCancer Atlas; <https://www.cancer.gov/tcga>] was chosen. This dataset from TCGA contains whole exome sequencing data from 585 cases, and mRNA sequencing data from 300 cases of ovarian serous carcinoma. Genomic alteration, mRNA expression and survival data were analyzed via the cBioPortal website by submitting a query regarding CRFs, including *ARID1A*, AT-rich interaction domain 1B, actin-like protein 6A (*ACTL6A*), *SMARCA1*, *SMARCA2*, *SMARCA4*, *SMARCA5*, *SMARCB1*, *SMARCC1*, *SMARCC2*, *SMARCC3*, *SMARCC4*, *SMARCC5*, *SMARCC6*, *SMARCC7*, *SMARCC8*, *SMARCC9*, *SMARCC10*, *SMARCC11*, *SMARCC12*, *SMARCC13*, *SMARCC14*, *SMARCC15*, *SMARCC16*, *SMARCC17*, *SMARCC18*, *SMARCC19*, *SMARCC20*, *SMARCC21*, *SMARCC22*, *SMARCC23*, *SMARCC24*, *SMARCC25*, *SMARCC26*, *SMARCC27*, *SMARCC28*, *SMARCC29*, *SMARCC30*, *SMARCC31*, *SMARCC32*, *SMARCC33*, *SMARCC34*, *SMARCC35*, *SMARCC36*, *SMARCC37*, *SMARCC38*, *SMARCC39*, *SMARCC40*, *SMARCC41*, *SMARCC42*, *SMARCC43*, *SMARCC44*, *SMARCC45*, *SMARCC46*, *SMARCC47*, *SMARCC48*, *SMARCC49*, *SMARCC50*, *SMARCC51*, *SMARCC52*, *SMARCC53*, *SMARCC54*, *SMARCC55*, *SMARCC56*, *SMARCC57*, *SMARCC58*, *SMARCC59*, *SMARCC60*, *SMARCC61*, *SMARCC62*, *SMARCC63*, *SMARCC64*, *SMARCC65*, *SMARCC66*, *SMARCC67*, *SMARCC68*, *SMARCC69*, *SMARCC70*, *SMARCC71*, *SMARCC72*, *SMARCC73*, *SMARCC74*, *SMARCC75*, *SMARCC76*, *SMARCC77*, *SMARCC78*, *SMARCC79*, *SMARCC80*, *SMARCC81*, *SMARCC82*, *SMARCC83*, *SMARCC84*, *SMARCC85*, *SMARCC86*, *SMARCC87*, *SMARCC88*, *SMARCC89*, *SMARCC90*, *SMARCC91*, *SMARCC92*, *SMARCC93*, *SMARCC94*, *SMARCC95*, *SMARCC96*, *SMARCC97*, *SMARCC98*, *SMARCC99*, *SMARCC100*, *SMARCC101*, *SMARCC102*, *SMARCC103*, *SMARCC104*, *SMARCC105*, *SMARCC106*, *SMARCC107*, *SMARCC108*, *SMARCC109*, *SMARCC110*, *SMARCC111*, *SMARCC112*, *SMARCC113*, *SMARCC114*, *SMARCC115*, *SMARCC116*, *SMARCC117*, *SMARCC118*, *SMARCC119*, *SMARCC120*, *SMARCC121*, *SMARCC122*, *SMARCC123*, *SMARCC124*, *SMARCC125*, *SMARCC126*, *SMARCC127*, *SMARCC128*, *SMARCC129*, *SMARCC130*, *SMARCC131*, *SMARCC132*, *SMARCC133*, *SMARCC134*, *SMARCC135*, *SMARCC136*, *SMARCC137*, *SMARCC138*, *SMARCC139*, *SMARCC140*, *SMARCC141*, *SMARCC142*, *SMARCC143*, *SMARCC144*, *SMARCC145*, *SMARCC146*, *SMARCC147*, *SMARCC148*, *SMARCC149*, *SMARCC150*, *SMARCC151*, *SMARCC152*, *SMARCC153*, *SMARCC154*, *SMARCC155*, *SMARCC156*, *SMARCC157*, *SMARCC158*, *SMARCC159*, *SMARCC160*, *SMARCC161*, *SMARCC162*, *SMARCC163*, *SMARCC164*, *SMARCC165*, *SMARCC166*, *SMARCC167*, *SMARCC168*, *SMARCC169*, *SMARCC170*, *SMARCC171*, *SMARCC172*, *SMARCC173*, *SMARCC174*, *SMARCC175*, *SMARCC176*, *SMARCC177*, *SMARCC178*, *SMARCC179*, *SMARCC180*, *SMARCC181*, *SMARCC182*, *SMARCC183*, *SMARCC184*, *SMARCC185*, *SMARCC186*, *SMARCC187*, *SMARCC188*, *SMARCC189*, *SMARCC190*, *SMARCC191*, *SMARCC192*, *SMARCC193*, *SMARCC194*, *SMARCC195*, *SMARCC196*, *SMARCC197*, *SMARCC198*, *SMARCC199*, *SMARCC200*, *SMARCC201*, *SMARCC202*, *SMARCC203*, *SMARCC204*, *SMARCC205*, *SMARCC206*, *SMARCC207*, *SMARCC208*, *SMARCC209*, *SMARCC210*, *SMARCC211*, *SMARCC212*, *SMARCC213*, *SMARCC214*, *SMARCC215*, *SMARCC216*, *SMARCC217*, *SMARCC218*, *SMARCC219*, *SMARCC220*, *SMARCC221*, *SMARCC222*, *SMARCC223*, *SMARCC224*, *SMARCC225*, *SMARCC226*, *SMARCC227*, *SMARCC228*, *SMARCC229*, *SMARCC230*, *SMARCC231*, *SMARCC232*, *SMARCC233*, *SMARCC234*, *SMARCC235*, *SMARCC236*, *SMARCC237*, *SMARCC238*, *SMARCC239*, *SMARCC240*, *SMARCC241*, *SMARCC242*, *SMARCC243*, *SMARCC244*, *SMARCC245*, *SMARCC246*, *SMARCC247*, *SMARCC248*, *SMARCC249*, *SMARCC250*, *SMARCC251*, *SMARCC252*, *SMARCC253*, *SMARCC254*, *SMARCC255*, *SMARCC256*, *SMARCC257*, *SMARCC258*, *SMARCC259*, *SMARCC260*, *SMARCC261*, *SMARCC262*, *SMARCC263*, *SMARCC264*, *SMARCC265*, *SMARCC266*, *SMARCC267*, *SMARCC268*, *SMARCC269*, *SMARCC270*, *SMARCC271*, *SMARCC272*, *SMARCC273*, *SMARCC274*, *SMARCC275*, *SMARCC276*, *SMARCC277*, *SMARCC278*, *SMARCC279*, *SMARCC280*, *SMARCC281*, *SMARCC282*, *SMARCC283*, *SMARCC284*, *SMARCC285*, *SMARCC286*, *SMARCC287*, *SMARCC288*, *SMARCC289*, *SMARCC290*, *SMARCC291*, *SMARCC292*, *SMARCC293*, *SMARCC294*, *SMARCC295*, *SMARCC296*, *SMARCC297*, *SMARCC298*, *SMARCC299*, *SMARCC300*, *SMARCC301*, *SMARCC302*, *SMARCC303*, *SMARCC304*, *SMARCC305*, *SMARCC306*, *SMARCC307*, *SMARCC308*, *SMARCC309*, *SMARCC310*, *SMARCC311*, *SMARCC312*, *SMARCC313*, *SMARCC314*, *SMARCC315*, *SMARCC316*, *SMARCC317*, *SMARCC318*, *SMARCC319*, *SMARCC320*, *SMARCC321*, *SMARCC322*, *SMARCC323*, *SMARCC324*, *SMARCC325*, *SMARCC326*, *SMARCC327*, *SMARCC328*, *SMARCC329*, *SMARCC330*, *SMARCC331*, *SMARCC332*, *SMARCC333*, *SMARCC334*, *SMARCC335*, *SMARCC336*, *SMARCC337*, *SMARCC338*, *SMARCC339*, *SMARCC340*, *SMARCC341*, *SMARCC342*, *SMARCC343*, *SMARCC344*, *SMARCC345*, *SMARCC346*, *SMARCC347*, *SMARCC348*, *SMARCC349*, *SMARCC350*, *SMARCC351*, *SMARCC352*, *SMARCC353*, *SMARCC354*, *SMARCC355*, *SMARCC356*, *SMARCC357*, *SMARCC358*, *SMARCC359*, *SMARCC360*, *SMARCC361*, *SMARCC362*, *SMARCC363*, *SMARCC364*, *SMARCC365*, *SMARCC366*, *SMARCC367*, *SMARCC368*, *SMARCC369*, *SMARCC370*, *SMARCC371*, *SMARCC372*, *SMARCC373*, *SMARCC374*, *SMARCC375*, *SMARCC376*, *SMARCC377*, *SMARCC378*, *SMARCC379*, *SMARCC380*, *SMARCC381*, *SMARCC382*, *SMARCC383*, *SMARCC384*, *SMARCC385*, *SMARCC386*, *SMARCC387*, *SMARCC388*, *SMARCC389*, *SMARCC390*, *SMARCC391*, *SMARCC392*, *SMARCC393*, *SMARCC394*, *SMARCC395*, *SMARCC396*, *SMARCC397*, *SMARCC398*, *SMARCC399*, *SMARCC400*, *SMARCC401*, *SMARCC402*, *SMARCC403*, *SMARCC404*, *SMARCC405*, *SMARCC406*, *SMARCC407*, *SMARCC408*, *SMARCC409*, *SMARCC410*, *SMARCC411*, *SMARCC412*, *SMARCC413*, *SMARCC414*, *SMARCC415*, *SMARCC416*, *SMARCC417*, *SMARCC418*, *SMARCC419*, *SMARCC420*, *SMARCC421*, *SMARCC422*, *SMARCC423*, *SMARCC424*, *SMARCC425*, *SMARCC426*, *SMARCC427*, *SMARCC428*, *SMARCC429*, *SMARCC430*, *SMARCC431*, *SMARCC432*, *SMARCC433*, *SMARCC434*, *SMARCC435*, *SMARCC436*, *SMARCC437*, *SMARCC438*, *SMARCC439*, *SMARCC440*, *SMARCC441*, *SMARCC442*, *SMARCC443*, *SMARCC444*, *SMARCC445*, *SMARCC446*, *SMARCC447*, *SMARCC448*, *SMARCC449*, *SMARCC450*, *SMARCC451*, *SMARCC452*, *SMARCC453*, *SMARCC454*, *SMARCC455*, *SMARCC456*, *SMARCC457*, *SMARCC458*, *SMARCC459*, *SMARCC460*, *SMARCC461*, *SMARCC462*, *SMARCC463*, *SMARCC464*, *SMARCC465*, *SMARCC466*, *SMARCC467*, *SMARCC468*, *SMARCC469*, *SMARCC470*, *SMARCC471*, *SMARCC472*, *SMARCC473*, *SMARCC474*, *SMARCC475*, *SMARCC476*, *SMARCC477*, *SMARCC478*, *SMARCC479*, *SMARCC480*, *SMARCC481*, *SMARCC482*, *SMARCC483*, *SMARCC484*, *SMARCC485*, *SMARCC486*, *SMARCC487*, *SMARCC488*, *SMARCC489*, *SMARCC490*, *SMARCC491*, *SMARCC492*, *SMARCC493*, *SMARCC494*, *SMARCC495*, *SMARCC496*, *SMARCC497*, *SMARCC498*, *SMARCC499*, *SMARCC500*, *SMARCC501*, *SMARCC502*, *SMARCC503*, *SMARCC504*, *SMARCC505*, *SMARCC506*, *SMARCC507*, *SMARCC508*, *SMARCC509*, *SMARCC510*, *SMARCC511*, *SMARCC512*, *SMARCC513*, *SMARCC514*, *SMARCC515*, *SMARCC516*, *SMARCC517*, *SMARCC518*, *SMARCC519*, *SMARCC520*, *SMARCC521*, *SMARCC522*, *SMARCC523*, *SMARCC524*, *SMARCC525*, *SMARCC526*, *SMARCC527*, *SMARCC528*, *SMARCC529*, *SMARCC530*, *SMARCC531*, *SMARCC532*, *SMARCC533*, *SMARCC534*, *SMARCC535*, *SMARCC536*, *SMARCC537*, *SMARCC538*, *SMARCC539*, *SMARCC540*, *SMARCC541*, *SMARCC542*, *SMARCC543*, *SMARCC544*, *SMARCC545*, *SMARCC546*, *SMARCC547*, *SMARCC548*, *SMARCC549*, *SMARCC550*, *SMARCC551*, *SMARCC552*, *SMARCC553*, *SMARCC554*, *SMARCC555*, *SMARCC556*, *SMARCC557*, *SMARCC558*, *SMARCC559*, *SMARCC560*, *SMARCC561*, *SMARCC562*, *SMARCC563*, *SMARCC564*, *SMARCC565*, *SMARCC566*, *SMARCC567*, *SMARCC568*, *SMARCC569*, *SMARCC570*, *SMARCC571*, *SMARCC572*, *SMARCC573*, *SMARCC574*, *SMARCC575*, *SMARCC576*, *SMARCC577*, *SMARCC578*, *SMARCC579*, *SMARCC580*, *SMARCC581*, *SMARCC582*, *SMARCC583*, *SMARCC584*, *SMARCC585*, *SMARCC586*, *SMARCC587*, *SMARCC588*, *SMARCC589*, *SMARCC590*, *SMARCC591*, *SMARCC592*, *SMARCC593*, *SMARCC594*, *SMARCC595*, *SMARCC596*, *SMARCC597*, *SMARCC598*, *SMARCC599*, *SMARCC600*, *SMARCC601*, *SMARCC602*, *SMARCC603*, *SMARCC604*, *SMARCC605*, *SMARCC606*, *SMARCC607*, *SMARCC608*, *SMARCC609*, *SMARCC610*, *SMARCC611*, *SMARCC612*, *SMARCC613*, *SMARCC614*, *SMARCC615*, *SMARCC616*, *SMARCC617*, *SMARCC618*, *SMARCC619*, *SMARCC620*, *SMARCC621*, *SMARCC622*, *SMARCC623*, *SMARCC624*, *SMARCC625*, *SMARCC626*, *SMARCC627*, *SMARCC628*, *SMARCC629*, *SMARCC630*, *SMARCC631*, *SMARCC632*, *SMARCC633*, *SMARCC634*, *SMARCC635*, *SMARCC636*, *SMARCC637*, *SMARCC638*, *SMARCC639*, *SMARCC640*, *SMARCC641*, *SMARCC642*, *SMARCC643*, *SMARCC644*, *SMARCC645*, *SMARCC646*, *SMARCC647*, *SMARCC648*, *SMARCC649*, *SMARCC650*, *SMARCC651*, *SMARCC652*, *SMARCC653*, *SMARCC654*, *SMARCC655*, *SMARCC656*, *SMARCC657*, *SMARCC658*, *SMARCC659*, *SMARCC660*, *SMARCC661*, *SMARCC662*, *SMARCC663*, *SMARCC664*, *SMARCC665*, *SMARCC666*, *SMARCC667*, *SMARCC668*, *SMARCC669*, *SMARCC670*, *SMARCC671*, *SMARCC672*, *SMARCC673*, *SMARCC674*, *SMARCC675*, *SMARCC676*, *SMARCC677*, *SMARCC678*, *SMARCC679*, *SMARCC680*, *SMARCC681*, *SMARCC682*, *SMARCC683*, *SMARCC684*, *SMARCC685*, *SMARCC686*, *SMARCC687*, *SMARCC688*, *SMARCC689*, *SMARCC690*, *SMARCC691*, *SMARCC692*, *SMARCC693*, *SMARCC694*, *SMARCC695*, *SMARCC696*, *SMARCC697*, *SMARCC698*, *SMARCC699*, *SMARCC700*, *SMARCC701*, *SMARCC702*, *SMARCC703*, *SMARCC704*, *SMARCC705*, *SMARCC706*, *SMARCC707*, *SMARCC708*, *SMARCC709*, *SMARCC710*, *SMARCC711*, *SMARCC712*, *SMARCC713*, *SMARCC714*, *SMARCC715*, *SMARCC716*, *SMARCC717*, *SMARCC718*, *SMARCC719*, *SMARCC720*, *SMARCC721*, *SMARCC722*, *SMARCC723*, *SMARCC724*, *SMARCC725*, *SMARCC726*, *SMARCC727*, *SMARCC728*, *SMARCC729*, *SMARCC730*, *SMARCC731*, *SMARCC732*, *SMARCC733*, *SMARCC734*, *SMARCC735*, *SMARCC736*, *SMARCC737*, *SMARCC738*, *SMARCC739*, *SMARCC740*, *SMARCC741*, *SMARCC742*, *SMARCC743*, *SMARCC744*, *SMARCC745*, *SMARCC746*, *SMARCC747*, *SMARCC748*, *SMARCC749*, *SMARCC750*, *SMARCC751*, *SMARCC752*, *SMARCC753*, *SMARCC754*, *SMARCC755*, *SMARCC756*, *SMARCC757*, *SMARCC758*, *SMARCC759*, *SMARCC760*, *SMARCC761*, *SMARCC762*, *SMARCC763*, *SMARCC764*, *SMARCC765*, *SMARCC766*, *SMARCC767*, *SMARCC768*, *SMARCC769*, *SMARCC770*, *SMARCC771*, *SMARCC772*, *SMARCC773*, *SMARCC774*, *SMARCC775*, *SMARCC776*, *SMARCC777*, *SMARCC778*, *SMARCC779*, *SMARCC780*, *SMARCC781*, *SMARCC782*, *SMARCC783*, *SMARCC784*, *SMARCC785*, *SMARCC786*, *SMARCC787*, *SMARCC788*, *SMARCC789*, *SMARCC790*, *SMARCC791*, *SMARCC792*, *SMARCC793*, *SMARCC794*, *SMARCC795*, *SMARCC796*, *SMARCC797*, *SMARCC798*, *SMARCC799*, *SMARCC800*, *SMARCC801*, *SMARCC802*, *SMARCC803*, *SMARCC804*, *SMARCC805*, *SMARCC806*, *SMARCC807*, *SMARCC808*, *SMARCC809*, *SMARCC810*, *SMARCC811*, *SMARCC812*, *SMARCC813*, *SMARCC814*, *SMARCC815*, *SMARCC816*, *SMARCC817*, *SMARCC818*, *SMARCC819*, *SMARCC820*, *SMARCC821*, *SMARCC822*, *SMARCC823*, *SMARCC824*, *SMARCC825*, *SMARCC826*, *SMARCC827*, *SMARCC828*, *SMARCC829*, *SMARCC830*, *SMARCC831*, *SMARCC832*, *SMARCC833*, *SMARCC834*, *SMARCC835*, *SMARCC836*, *SMARCC837*, *SMARCC838*, *SMARCC839*, *SMARCC840*, *SMARCC841*, *SMARCC842*, *SMARCC843*, *SMARCC844*, *SMARCC845*, *SMARCC846*, *SMARCC847*, *SMARCC848*, *SMARCC849*, *SMARCC850*, *SMARCC851*, *SMARCC852*, *SMARCC853*, *SMARCC854*, *SMARCC855*, *SMARCC856*, *SMARCC857*, *SMARCC858*, *SMARCC859*, *SMARCC860*, *SMARCC861*, *SMARCC862*, *SMARCC863*, *SMARCC864*, *SMARCC865*, *SMARCC866*, *SMARCC867*, *SMARCC868*, *SMARCC869*, *SMARCC870*, *SMARCC871*, *SMARCC872*, *SMARCC873*, *SMARCC874*, *SMARCC875*, *SMARCC876*, *SMARCC877*, *SMARCC878*, *SMARCC879*, *SMARCC880*, *SMARCC881*, *SMARCC882*, *SMARCC883*, *SMARCC884*, *SMARCC885*, *SMARCC886*, *SMARCC887*, *SMARCC888*, *SMARCC889*, *SMARCC890*, *SMARCC891*, *SMARCC892*, *SMARCC893*, *SMARCC894*, *SMARCC895*, *SMARCC896*, *SMARCC897*, *SMARCC898*, *SMARCC899*, *SMARCC900*, *SMARCC901*, *SMARCC902*, *SMARCC903*, *SMARCC904*, *SMARCC905*, *SMARCC906*, *SMARCC907*, *SMARCC908*, *SMARCC909*, *SMARCC910*, *SMARCC911*, *SMARCC912*, *SMARCC913*, *SMARCC914*, *SMARCC915*, *SMARCC916*, *SMARCC917*, *SMARCC918*, *SMARCC919*, *SMARCC920*, *SMARCC921*, *SMARCC922*, *SMARCC923*, *SMARCC924*, *SMARCC925*, *SMARCC926*, *SMARCC927*, *SMARCC928*, *SMARCC929*, *SMARCC930*, *SMARCC931*, *SMARCC932*, *SMARCC933*, *SMARCC934*, *SMARCC935*, *SMARCC936*, *SMARCC937*, *SMARCC938*, *SMARCC939*, *SMARCC940*, *SMARCC941*, *SMARCC942*, *SMARCC943*, *SMARCC944*, *SMARCC945*, *SMARCC946*, *SMARCC947*, *SMARCC948*, *SMARCC949*, *SMARCC950*, *SMARCC951*, *SMARCC952*, *SMARCC953*, *SMARCC954*, *SMARCC955*, *SMARCC956*, *SMARCC957*, *SMARCC958*, *SMARCC959*, *SMARCC960*, *SMARCC961*, *SMARCC962*, *SMARCC963*, *SMARCC964*, *SMARCC965*, *SMARCC966*, *SMARCC967*, *SMAR*

manufacturer's instructions. Sections were dehydrated in an ethanol series (95, 99 and 100%) and cleared in xylene. Nuclear staining of stromal cells and vascular endothelium was used as a positive internal control and stroma was used as a negative internal control to evaluate the staining. In several cases, p53 immunostaining was performed to support histological diagnosis. The evaluation of IHC slides was conducted using a light microscope by two pathologists (NM and TI) who were blinded to the details of the patients.

Immunohistochemical scoring. The expression of ARID1A, SMARCA2, SMARCA4, SMARCB1, SMARCC2 and H3K27me3 was considered 'lost' when there was a complete absence of nuclear staining in tumor cells, while the surrounding normal cells exhibited consistently preserved nuclear staining. By contrast, ACTL6A, SMARCC2 and CHD4 expression were evaluated using an H-score, calculated by multiplying the proportion and intensity of tumor cells displaying nuclear staining. The proportion score was determined by assessing the percentage of tumor cells with positive nuclear staining relative to all tumor cells on the slide (0-100%). The intensity score was assessed using the intensity of the nuclear staining, categorized as follows: 0, not stained; 1, weak; 2, moderate; and 3, strong. The resulting H-score ranged from 0-300. The threshold value between the high and low protein expression groups was determined using the median H-score. Notably, stromal cells and vascular endothelium exhibited positivity and served as internal positive controls across all cases.

Copy number assay. Tumor DNA from each of the 203 cases was extracted from FFPE blocks using the DNASTORM FFPE Kit (Biotium, Inc.), according to the manufacturer's protocol. However, the copy number assay could not be conducted in some cases due to limited sample volume. Tumor DNA was successfully extracted in 154 cases for ACTL6A, 143 cases for SMARCC2 and 140 cases for CHD4. Normal DNA extracted from a normal skeletal muscle tissue was used as the control. TaqMan™ Copy Number Assay (cat. no. 4400291; Thermo Fisher Scientific Inc.) was used to conduct DNA copy number analysis. A pre-designed primer and probe mix specific for ACTL6A (Assay ID. Hs02294862_cn), SMARCC2 (Assay ID. Hs02933711_cn) and CHD4 (Assay ID. Hs02108296_cn) was used according to the manufacturer's instructions (Thermo Fisher Scientific Inc.). The *Rnase P* gene (cat. no. 4316844; Thermo Fisher Scientific Inc.) was used as the endogenous control. Quantitative polymerase chain reaction (qPCR) was performed with THUNDERBIRD™ Probe qPCR Mix (Toyobo Life Science) using the Δ Cq method (18) on a QuantStudio 3 Real Time PCR System (Thermo Fisher Scientific Inc.). The thermocycling conditions were as follows: Hot start at 50°C for 2 min and 95°C for 1 min; followed by 50 cycles of denaturation at 95°C for 15 sec, annealing at 60°C for 60 sec and extension at 68°C for 30 sec. The relative quantities of DNA obtained from the PCR were analyzed using CopyCaller (Thermo Fisher Scientific Inc.) to determine the copy numbers. Cases with negative results for *Rnase P* were excluded from the analysis. Copy number alterations (CNAs) were categorized as follows: Copy number <1, deep deletion; 1, shallow deletion; 2, diploid; 3-4, gain and >4, amplification.

Statistical analysis. All statistical analyses were performed using the JMP statistical software version 17 (SAS Institute, Inc.). The data were analyzed using Wilcoxon's rank-sum test. Multiple comparisons of DNA copy number data and immunohistochemical expression data were analyzed using the Wilcoxon rank-sum test with Bonferroni correction. For survival analysis, Kaplan-Meier analysis and the log-rank test were used. $P < 0.05$ was considered to indicate a statistically significant difference.

Results

Public data analysis. The gene alterations of CRFs in ovarian serous carcinoma are summarized in Fig. 1A. Among 585 cases, 57% demonstrated CRF gene alterations, primarily in the form of gene amplification, which was observed in 208 (35.6%) cases. The most prevalent genetic alteration among CRFs in ovarian serous carcinoma was ACTL6A amplification (19.5%). However, this genetic alteration did not significantly affect OS ($P = 0.620$; Fig. 1B). Patients with SMARCC2 amplification (3.1%) had a significantly shorter median OS compared with patients with unaltered SMARCC2 ($P = 0.005$; Fig. 1C). Patients with CHD4 amplification (5.7%) had a notably shorter OS compared with patients with unaltered CHD4; however, this association was not statistically significant ($P = 0.169$; Fig. 1D). Furthermore, there was no significant association between ACTL6A, SMARCC2 and CHD4 mRNA expression levels and OS (Fig. S1A-C). However, ACTL6A mRNA expression was significantly higher in patients with ACTL6A amplification compared with in patients without alterations in the ACTL6A gene ($P < 0.001$; Fig. S1D).

Clinicopathological data analysis. Table I presents the clinical characteristics of patients with OHGSC included in the present histological study. The age of the patients ranged from 28-87 years (mean, 58.3 years; median, 58 years). Out of the 203 cases, 148 (72.9%) had available 5-year clinical follow-up data, with a mean follow-up duration of 61.9 months (1-233 months). The majority of patients (78.4%) presented with advanced stage disease (III-IV). In total, there were 124 cases (61.1%) with recurrence, and 81 cases (39.9%) resulted in disease-related death.

Regarding treatment, all cases underwent surgical resection. Additionally, 195 cases (96.1%) received adjuvant chemotherapy, consisting of various regimens, such as paclitaxel and carboplatin, docetaxel and carboplatin, cyclophosphamide, doxorubicin and cisplatin, cyclophosphamide, epirubicin and cisplatin, or paclitaxel and cisplatin. Furthermore, 9 cases received maintenance treatment, which supplemented chemotherapy with bevacizumab treatment.

Immunohistochemical results. Figs. 2, S2 and S3 display representative images of IHC staining, while the summarized IHC results are presented in Table II. ARID1A, SMARCA2, SMARCA4, SMARCB1, SMARCC2 and H3K27me3 were predominantly expressed in the nucleus of the tumor cells (Fig. S2). Nuclear staining of CRFs was lost in 8.9% of cases. Specifically, loss of nuclear ARID1A staining occurred in 2.5% of cases, SMARCA2 in 2.5% of cases and SMARCA4

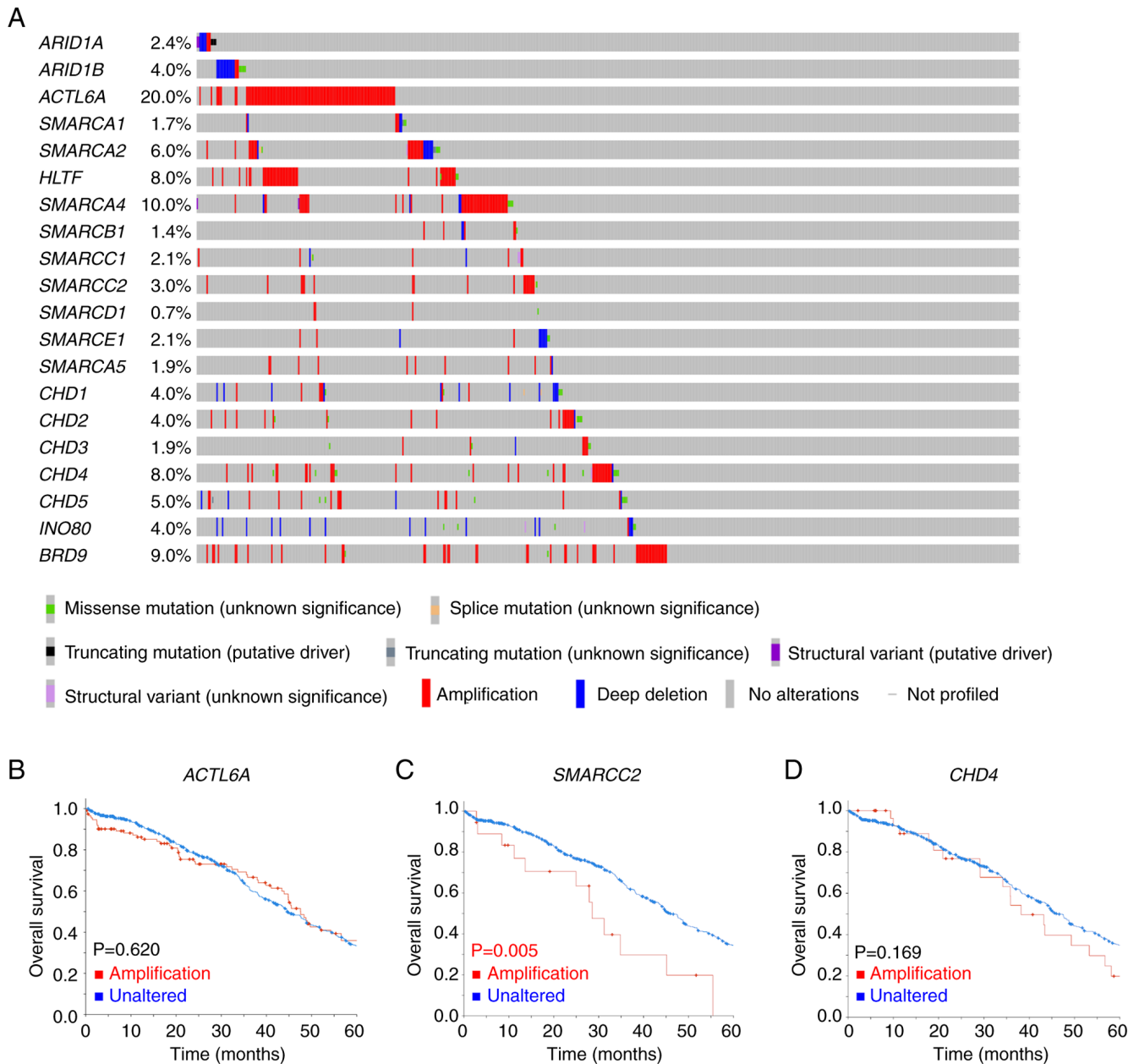


Figure 1. *SMARCC2* gene amplification is related to unfavorable prognosis in patients with ovarian serous carcinoma. (A) OncoPrint plot showing the genomic profile and frequency of genetic alterations in chromatin remodeling factors based on data from The Cancer Genome Atlas, as compiled by cBioPortal. Kaplan-Meier survival curves for overall survival based on the gene alteration status of (B) *ACTL6A*, (C) *SMARCC2* and (D) *CHD4*. *ACTL6A*, actin-like protein 6A; *SMARCC2*, switch/sucrose non-fermentable related, matrix associated, actin dependent regulator of chromatin subfamily c member 2; *CHD4*, chromodomain-helicase-DNA-binding protein 4.

in 3.9% of cases (Table II; Fig. 2A-C). Additionally, 2.5% of cases exhibited loss of H3K27me3 expression (Table II; Fig. 2D). The nuclear staining of these markers in stromal cells and vascular endothelium served as a positive internal control. Loss of ARID1A, SMARCA2 and SMARCA4 protein expression was mutually exclusive, and the loss of H3K27me3 was not related to loss of the protein expression of these CRFs. However, SMARCC2 and SMARCB1 protein expression was retained in all cases (Table II). The intensity of *ACTL6A*, *SMARCC2* and *CHD4* protein expression was higher in tumor cells compared with in stromal cells or lymphocytes (Fig. 2E-G). In addition, the nucleus of OHGSC tumor cells was strongly and diffusely positive for p53 (Fig. 2H).

The H-score of *ACTL6A*, *SMARCC2* and *CHD4* ranged from 140-220 (mean 169.66), 140-210 (mean 180.39), and 60-210 (mean 168.82), respectively. The median H-scores: 170 for *ACTL6A*, 180 for *SMARCC2* and 170 for *CHD4*, were used as the cutoff values for distinguishing low and high CRF expression; representative images of high and low *ACTL6A*, *SMARCC2* and *CHD4* staining are shown (Fig. S3A-F).

Copy number analysis. Fig. 3A presents a summary of the DNA copy numbers of *ACTL6A*, *SMARCC2* and *CHD4* in OHGSC. Results were obtained for 154 cases for *ACTL6A*, 143 cases for *SMARCC2* and 140 cases for *CHD4*, out of a total of 203 cases.

Table I. Clinicopathological features of patients with OHGSC (n=203).

Characteristic	No. (%)
FIGO stage	
I	21 (10.3)
II	23 (11.3)
III	114 (56.2)
IV	45 (22.2)
T stage	
1	30 (14.8)
2	37 (18.2)
3	136 (67.0)
N stage	
0	68 (33.5)
1	104 (51.2)
X	31 (15.3)
M stage	
0	158 (77.8)
1	45 (22.2)
Recurrence	
-	79 (38.9)
+	124 (61.1)
Adjuvant chemotherapy	
-	8 (3.9)
+	195 (96.1)
Tumor-related mortality	
NED	52 (25.6)
AWD	15 (7.4)
DOD	81 (39.9)
NA	55 (27.1)

NED, no evidence of disease; AWD, alive with disease; DOD, dead of disease; NA, not available; X, regional lymph node metastasis not evaluable.

For comparison, normal skeletal muscle tissue was used as the control and the copy numbers were normalized to *Rnase P*, which served as the internal control. The copy numbers of *ACTL6A*, *SMARCC2* and *CHD4* ranged from 1-8 (mean 3.09), 1-7 (mean 2.27), and 0-5 (mean 1.34), respectively.

Notably, CNAs with increased copy numbers were predominant in *ACTL6A* and *SMARCC2*, while *CHD4* CNAs primarily exhibited decreased copy numbers. Among the cases assessed, 102 out of 154 (66.2%) demonstrated *ACTL6A* copy number gain or gene amplification, 48 out of 143 (33.5%) showed *SMARCC2* copy number gain or gene amplification, and 99 out of 140 (70.7%) demonstrated *CHD4* shallow deletion or deep deletion. The relationship between *ACTL6A*, *SMARCC2* and *CHD4* copy numbers and the immunohistochemical expression of these proteins was assessed. However, no statistically significant association was observed between the copy numbers and the protein expression of *ACTL6A* (Fig. 3B), *SMARCC2* (Fig. 3C) and *CHD4* (Fig. 3D).

Table II. Immunohistochemistry results.

Antibody	Positivity	No. (%)
ARID1A	Lost	5/203 (2.5)
	Retained	198/203 (97.5)
SMARCA2	Lost	5/203 (2.5)
	Retained	198/203 (97.5)
SMARCA4	Lost	8/203 (3.9)
	Retained	195/203 (96.1)
SMARCB1	Lost	0/203 (0)
	Retained	203/203 (100)
SMARCC2	Lost	0/203 (0)
	Retained	203/203 (100)
H3K27me3	Lost	5/203 (2.5)
	Retained	198/203 (97.5)

ARID1A, AT-rich interaction domain 1A; SMAR, SWI/SNF related, matrix associated, actin dependent regulator of chromatin; SMARCA, SMARC subfamily a; SMARCB, SMARC subfamily b; SMARCC, SMARC subfamily c; H3K27me3, tri-methylation of lysine 27 of histone H3.

Relationship between prognosis and CRFs. The survival analyses for copy numbers of CRFs are summarized in Fig. S4, while the association of protein expression with OS is presented in Fig. 4.

Regarding the CNAs of *ACTL6A*, *SMARCC2* and *CHD4*, changes in copy number of these genes demonstrated no statistically significant association with the OS of patients (P=0.434, P=0.629 and P=0.578, respectively; Fig. S4A-C). Similarly, there was no significant association between the copy numbers of these CRFs and the FIGO stage (P=0.506, P=0.862 and P=0.974, respectively; Fig. S4D-F). However, although not significant (P=0.094), in patients with FIGO stage III/IV OHGSC, copy number gain or amplification in either *ACTL6A*, *SMARCC2* or *CHD4* demonstrated unfavorable outcome trends compared with patients with diploid *ACTL6A*, *SMARCC2* and *CHD4* (Fig. S4G).

Moreover, although not significant (P=0.128), patients with FIGO stage III/IV with shallow or deep deletions in either *ACTL6A*, *SMARCC2* or *CHD4* demonstrated unfavorable outcome trends compared with those with *ACTL6A*, *SMARCC2* and *CHD4* diploids (Fig. S4H). However, due to the small number of cases, the effect of CRF CNAs on FIGO stage I/II cases could not be analyzed.

In cases with decreased protein levels of ARID1A, SMARCA2 or SMARCA4, similar outcome trends were demonstrated in OS compared with those with retained expression levels, and there was no statistically significant difference (P=0.879; Fig. 4A). Notably, patients with high *ACTL6A* protein levels demonstrated a statistically longer OS compared with patients with low *ACTL6A* protein levels (P=0.027; Fig. 4B).

Regarding the association with FIGO stage, higher *SMARCC2* protein expression was detected in patients with a higher FIGO stage, but this relationship was not statistically significant (P=0.198; Fig. 4D). Likewise, the difference between *ACTL6A* and *CHD4* protein levels and FIGO stage

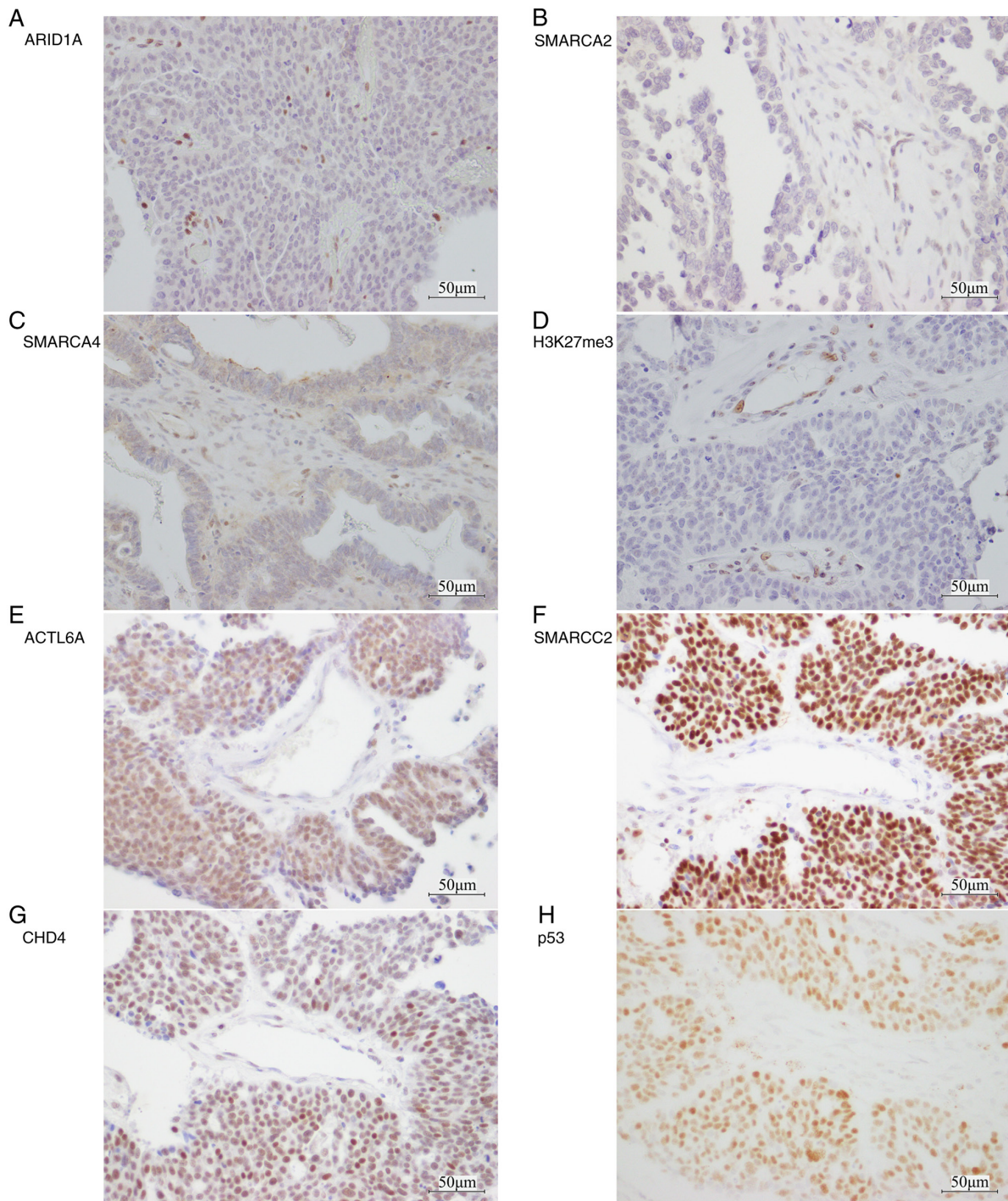


Figure 2. Representative immunohistochemistry images for chromatin remodeling factors and H3K27me3 in ovarian high-grade serous carcinoma. Loss of nuclear staining in tumor cells for (A) ARID1A, (B) SMARCA2, (C) SMARCA4 and (D) H3K27me3. (E) ACTL6A, (F) SMARCC2 and (G) CHD4 exhibited stronger nuclear expression in tumor cells compared with stromal cells and lymphocytes. Stromal cells and vascular endothelium demonstrated consistently preserved nuclear staining, serving as a positive internal control. (H) Aberrant expression of p53 in the nucleus of tumor cells. Scale bar, 50 μ m. ARID1A, AT-rich interaction domain 1A; SMARCA, switch/sucrose non-fermentable related, matrix associated, actin dependent regulator of chromatin subfamily a; H3K27me3, tri-methylation of lysine 27 of histone H3; ACTL6A, actin-like protein 6A; SMARCC2, switch/sucrose non-fermentable related, matrix associated, actin dependent regulator of chromatin subfamily c member 2; CHD4, chromodomain-helicase-DNA-binding protein 4.

was not found to be significantly different ($P=0.315$ and $P=0.775$, respectively; Fig. 4C and E).

Discussion

The present study conducted a comprehensive analysis of the relationship between CRF alterations and the

clinicopathological features of OHGSC. The findings revealed CNAs in ACTL6A, SMARCC2 and CHD4 in OHGSC, as well as protein loss of ARID1A (2.5%), SMARCA2 (2.5%) and SMARCA4 (3.9%), indicating possible gene alterations. Notably, low protein expression levels of ACTL6A were identified as a positive indicator of shortened OS in patients with OHGSC.

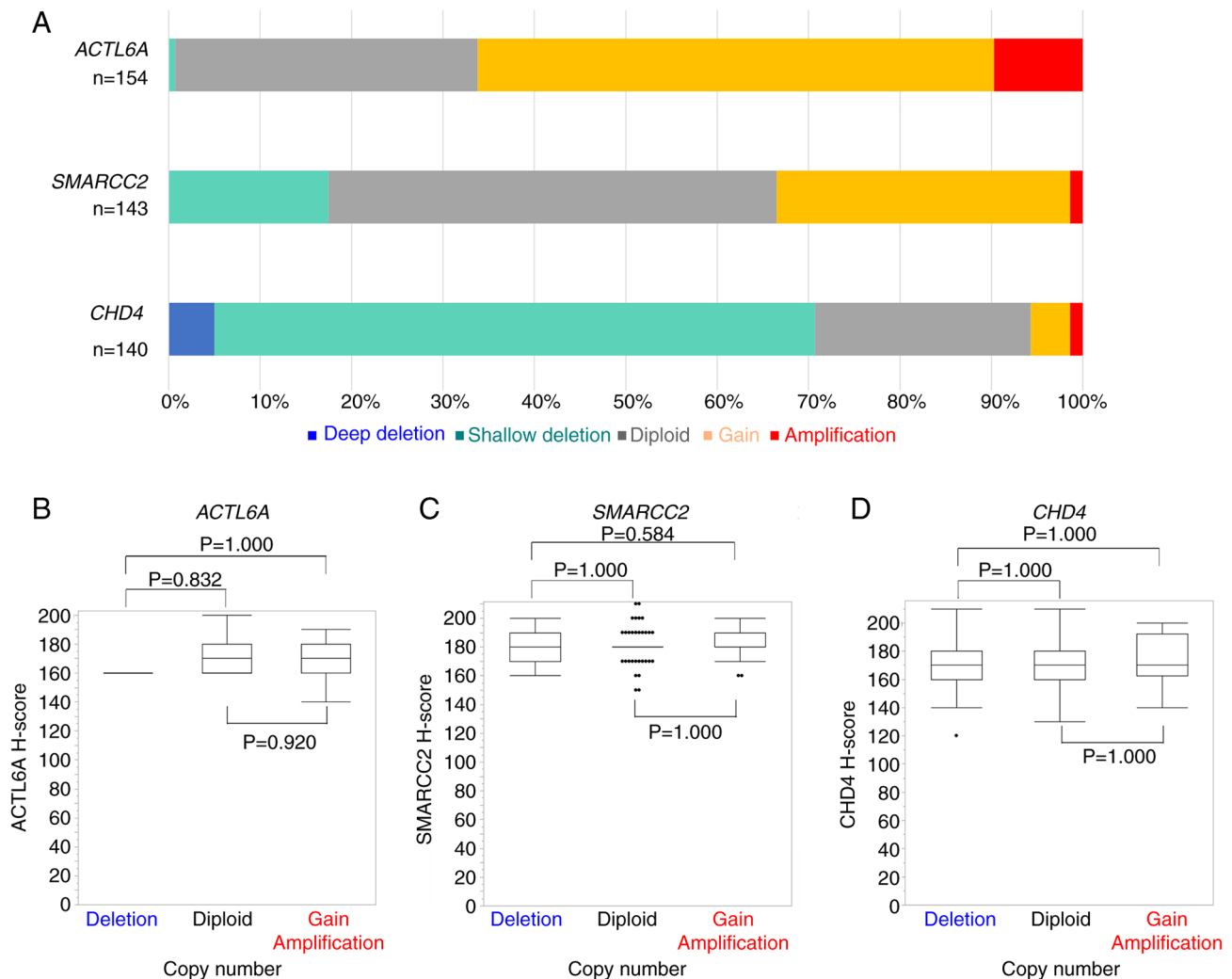


Figure 3. DNA copy number analysis of *ACTL6A*, *SMARCC2* and *CHD4* using the TaqMan copy number assay. (A) Copy numbers were primarily increased in *ACTL6A* and *SMARCC2* and decreased in *CHD4*; these values were normalized to the internal control *RNase P*. A total of 66.2% of cases exhibited *ACTL6A* copy number gain or gene amplification, 33.5% demonstrated *SMARCC2* copy number gain or gene amplification, and 70.7% displayed *CHD4* deep deletion or shallow deletion. The relationship between (B) *ACTL6A*, (C) *SMARCC2* and (D) *CHD4* copy numbers and their immunohistochemical expression. No statistically significant association was demonstrated between the different copy numbers and protein expression. *ACTL6A*, actin-like protein 6A; *SMARCC2*, switch/sucrose non-fermentable related, matrix associated, actin dependent regulator of chromatin subfamily c member 2; *CHD4*, chromodomain-helicase-DNA-binding protein 4.

Adenosine triphosphate (ATP)-dependent chromatin remodeling complexes regulate the chromatin packing state by sliding, ejecting and restructuring the nucleosome for transcriptional regulation (19). The Brg1-associated factor (BAF) complex is composed of a central ATPase (SMARCA2 or SMARCA4) and multiple BAFs, including ARID1A, *ACTL6A* and *SMARCC2*, which are assembled in a combinatorial fashion to dictate functional specificity (20). Overall, complex stoichiometry is influenced by individual BAFs that can regulate the expression of other subunits (21).

CHD4 is a core component of the nucleosome remodeling and deacetylase complex that combines chromatin remodeling activity with histone deacetylase and demethylase functions, which are involved in transcriptional repression (22). *CHD4* comprises a core ATPase/helicase domain flanked by two plant homeodomain motifs that recognize modifications of histone tails, tandem chromodomains and carboxyl-terminal domains (23).

Previous studies have highlighted the amplification and upregulation of *ACTL6A* in numerous types of cancer, such

as ovarian cancer, glioma, squamous cell carcinoma, osteosarcoma and hepatocellular carcinoma (24-28). *ACTL6A* has been implicated in promoting metastasis and epithelial-mesenchymal transition in hepatocellular carcinoma (28) and colon cancer (29). Additionally, it has been reported to serve a role in tumorigenesis in head and neck squamous cell carcinoma (26) and glioma (25) by activating the Hippo/YAP pathway. In the context of ovarian cancer, high mRNA expression of *ACTL6A* has been reported to be associated with shortened OS (24) and platinum resistance (30). In the present study, public data demonstrated no significant association between *ACTL6A* mRNA expression and prognosis in patients with ovarian serous carcinoma; however, low *ACTL6A* protein expression levels, as detected by IHC, were associated with decreased OS. Thus, the protein levels and mRNA levels may not be comparable. Differences between mRNA and protein levels may arise due to technical or biological reasons, such as post-transcriptional regulation (31). The process of mRNA stabilization needs to be elucidated to prove these divergences.

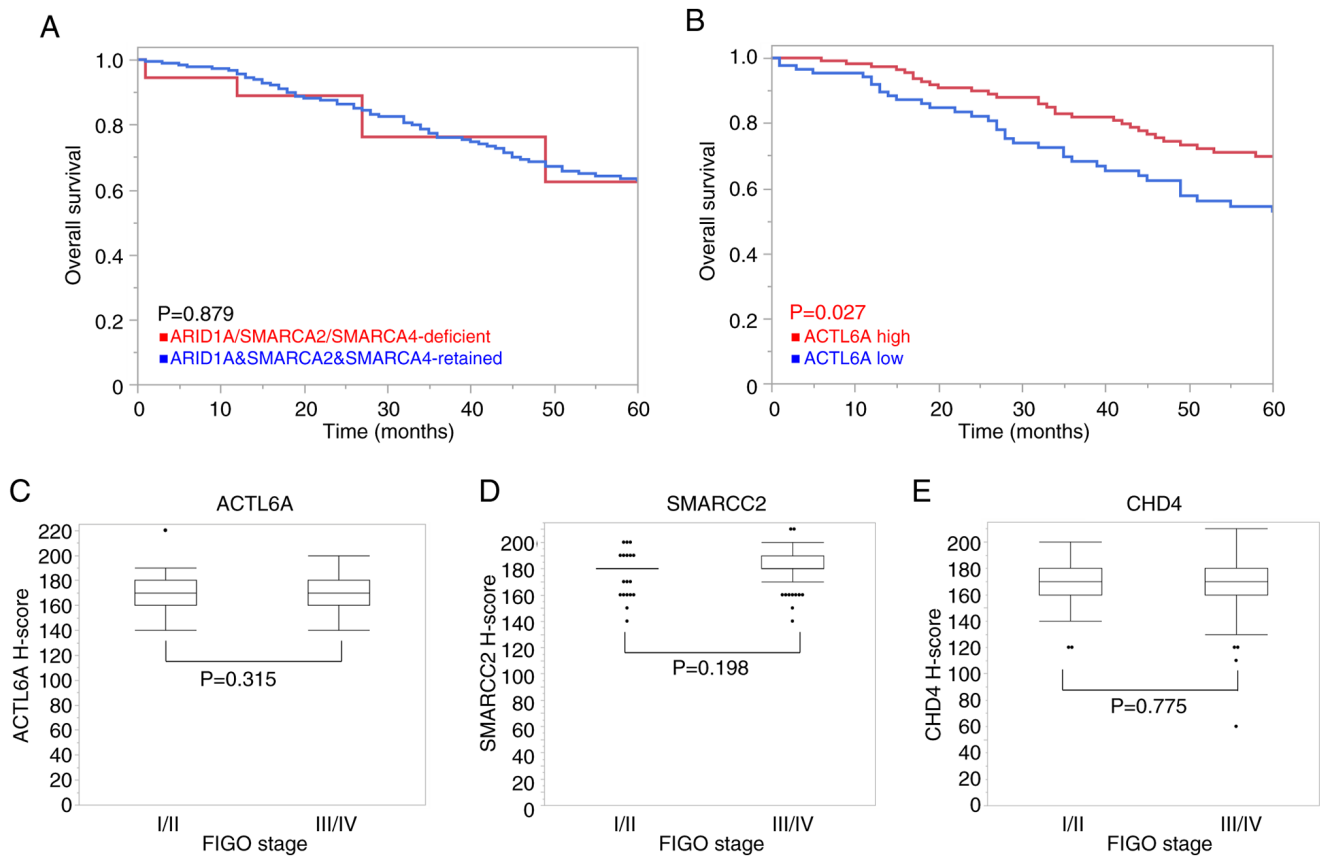


Figure 4. Relationship among CRF protein expression, overall survival and clinical stages in patients with OHGSC. (A) Kaplan-Meier survival analysis was performed for patients with a deficiency of any of the ARID1A, SMARCA2 and SMARCA4 protein levels or with retained protein levels. Cases with a deficiency of any of the ARID1A, SMARCA2 or SMARCA4 proteins demonstrated similar outcome trends compared with those with retained expression, and there was no statistically significant difference. (B) Kaplan-Meier analysis demonstrated the prognostic differences based on ACTL6A protein expression. Patients with high ACTL6A protein expression exhibited a more favorable outcome compared with those with low ACTL6A expression. The threshold value between the high and low groups was determined by the median H-score, 170. The relationship between (C) ACTL6A, (D) SMARCC2 and (E) CHD4 protein expression levels and the FIGO stage. (D) Patients with higher FIGO stage tended to have higher SMARCC2 expression, but this was not statistically significant. (C) ACTL6A and (E) CHD4 protein levels were unchanged between the FIGO stages. CRF, chromatin remodeling factor; OHGSC, ovarian high-grade serous carcinoma; FIGO, International Federation of Gynecology and Obstetrics; ARID1A, AT-rich interaction domain 1A; SMARCA, switch/sucrose non-fermentable related, matrix associated, actin dependent regulator of chromatin subfamily a; ACTL6A, actin-like protein 6A; SMARCC2, switch/sucrose non-fermentable related, matrix associated, actin dependent regulator of chromatin subfamily c member 2; CHD4, chromodomain-helicase-DNA-binding protein 4.

Additionally, despite a *ACTL6A* copy number gain or gene amplification in 66.2% of the cases tested, a statistically significant association between the copy number and protein levels of ACTL6A was not found. The different steps in the gene expression pathway each involve a complex process that confers regulatory control. Likewise, other epigenetic factors, such as microRNAs and ubiquitination, may have contributed to ACTL6A protein expression. Moreover, ACTL6A may affect the expression of oncogenes although *ACTL6A* mRNA expression was not related to prognosis. According to the present results, poor prognosis may be caused by the dysregulated transcription of other oncogenes or tumor suppressor genes following the decrease in ACTL6A protein expression. *In vitro* or *in vivo* analysis using protein knockdown or gene knockout of *ACTL6A* may be required to evaluate these hypotheses.

In the present study, it was demonstrated that patients with a higher FIGO stage tended to exhibit higher SMARCC2 protein expression. Furthermore, the analysis of TCGA data demonstrated that patients with *SMARCC2* amplification had a shorter median OS compared with patients with wild-type

SMARCC2 in ovarian serous carcinoma. Several studies have indicated that SMARCC2 is deficiently expressed in cancer (32,33). SMARCC2 has been reported to inhibit tumor development by mediating the expression of the transcription factor early growth response 1 via chromatin remodeling, and by inhibiting activation of the phosphoinositide 3-kinase-AKT pathway in glioblastoma (33). However, several studies have reported *SMARCC2* gene amplification in cancer, such as follicular lymphoma (34) and hepatocellular carcinoma (35), in line with the results of the present study. These results collectively suggested that SMARCC2 function varies according to tumor type, and that aberrant SMARCC2 expression could be involved in the regulation of numerous cellular functions, such as cell proliferation and the cell cycle of the tumor.

Additionally, patients in FIGO stage III/IV who have copy number gain or amplification in either *ACTL6A*, *SMARCC2* or *CHD4* had a poor prognosis compared with those of *ACTL6A*, *SMARCC2* and *CHD4* diploids.

In the present study, 8.9% of cases exhibited a deficiency in either ARID1A, SMARCA2 or SMARCA4 protein levels. Notably, the deficiency in ARID1A, SMARCA2 and

SMARCA4 was found to be mutually exclusive in this analysis. This exclusivity is attributed to the biochemical and functional heterogeneity of BAF complexes (36), and numerous epigenetic mechanisms are involved in the instability and silencing of SMARCA2, SMARCA4 and other subunits of the BAF complex (37). The BAF-chromatin remodeling complex, with its mutually exclusive ATPases SMARCA2 and SMARCA4, is essential for the transcriptional activation of numerous genes (38).

Furthermore, changes in nucleosome distribution pattern and density have been linked to reduced levels of H3K27me3 in chromatin remodeling enzyme mutants (39). However, in the present study, the loss of H3K27me3 was not found to be associated with the loss of CRFs expression.

The molecular biology of OHGSC is characterized by genomic complexity, often lacking targetable oncogenic alterations (40). Nonetheless, the present study revealed aberrant protein expression and CNAs of CRFs in OHGSC, which supports their potential use as therapeutic targets.

One limitation of the present study is the lack of *in vivo* confirmation of CRF expression in OHGSC. Thus, future studies using animal models are required to validate these findings.

There are ongoing developments in drugs that target genomic abnormalities of CRFs and combination therapies aimed at enhancing the therapeutic effects of anticancer drugs (41). In a previous study, the histone deacetylase inhibitor romidepsin, which targets CHD4, was demonstrated to suppress the progression of metastases in ovarian cancer both *in vitro* and *in vivo* (42). Additionally, panobinostat was reported to counteract ACTL6A-induced cisplatin resistance by inhibiting the repair of cisplatin-DNA adducts *in vivo* (30).

In conclusion, the present study demonstrated copy number and protein expression alterations of CRFs in OHGSC. Notably, the protein expression levels of ACTL6A were found to be associated with poor prognosis. These findings suggested that CRFs could be prognostic markers for OHGSC. However, further research is required to fully understand the mechanisms through which CRFs contribute to transcriptional aberration of oncogenes, particularly in the context of other epigenetic factors in OHGSC, and to investigate whether they are potential therapeutic targets for OHGSC.

Acknowledgements

The authors would like to thank Ms. Haruka Toki, Ms. Nahoko Ieiri, Ms. Jumi Yahiro, Ms. Motoko Tomita and Ms. Mami Nakamizo (Department of Anatomic Pathology, Kyushu University), for their technical support for this study.

Funding

This study received financial support from the 'FUKUOKA' OBGYN Researcher's Charity Foundation Fund, Japan, through grants-in-aid.

Availability of data and materials

The data generated in the present study may be found in The Cancer Genome Atlas or at the following URL: <https://www.cancer.gov/tcga>.

The other data generated in the present study may be requested from the corresponding author.

Authors' contributions

NM and TI conducted the research and wrote the article. KK, YK, TT, MN and FN contributed to the sample collection and research design. YO designed the research and gave final approval of the article. NM, TI and YO confirm the authenticity of all the raw data. All authors read and approved the final manuscript.

Ethics approval and consent to participate

This study was conducted in accordance with the principles of The Declaration of Helsinki. The study protocol was approved by the Ethics Committee of Kyushu University (Fukuoka, Japan; approval nos. 21120-01, 21037-02 and 23005-00). There was an opt-out approach for consent where participants were informed of the trial on the homepage and were invited to opt-out if preferred.

Patient consent for publication

Not applicable.

Competing interests

The authors declare that they have no competing interests.

References

- Kim J, Park EY, Kim O, Schilder JM, Coffey DM, Cho CH and Bast RC Jr: Cell origins of high-grade serous ovarian cancer. *Cancers (Basel)* 10: 433, 2018.
- Peres LC, Cushing-Haugen KL, Köbel M, Harris HR, Berchuck A, Rossing MA, Schidkrait JM and Doherty JA: Invasive epithelial ovarian cancer survival by histotype and disease stage. *J Natl Cancer Inst* 111: 60-68, 2019.
- Barlin JN, Long KC, Tanner EJ, Gardner GJ, Leitao MM Jr, Levine DA, Sonoda Y, Abu-Rustum NR, Barakat RR and Chi DS: Optimal (≤ 1 cm) but visible residual disease: Is extensive debulking warranted? *Gynecol Oncol* 130: 284-288, 2013.
- Dao F, Schlappe BA, Tseng J, Lester J, Nick AM, Lutgendorf SK, McMeekin S, Coleman RL, Moore KN, Karlan BY, *et al*: Characteristics of 10-year survivors of high-grade serous ovarian carcinoma. *Gynecol Oncol* 141: 260-263, 2016.
- Iacobuzio-Donahue CA: Epigenetic changes in cancer. *Annu Rev Pathol* 4: 229-249, 2009.
- Baylin SB and Jones PA: Epigenetic determinants of cancer. *Cold Spring Harb Perspect Biol* 8: a019505, 2016.
- Hasan N and Ahuja N: The emerging roles of ATP-dependent chromatin remodeling complexes in pancreatic cancer. *Cancers (Basel)* 11: 1859, 2019.
- Kadoch C and Crabtree GR: Mammalian SWI/SNF chromatin remodeling complexes and cancer: Mechanistic insights gained from human genomics. *Sci Adv* 1: e1500447, 2015.
- Khalique S, Naidoo K, Attygalle AD, Kriplani D, Daley F, Lowe A, Campbell J, Jones T, Hubank M, Fenwick K, *et al*: Optimised ARID1A immunohistochemistry is an accurate predictor of ARID1A mutational status in gynaecological cancers. *Pathol Clin Res* 4: 154-166, 2018.
- Le Gallo M, O'Hara AJ, Rudd ML, Urick ME, Hansen NF, O'Neil NJ, Price JC, Zhang S, England BM, Godwin AK, *et al*: Exome sequencing of serous endometrial tumors identifies recurrent somatic mutations in chromatin-remodeling and ubiquitin ligase complex genes. *Nat Genet* 44: 1310-1315, 2012.
- Wiegand KC, Shah SP, Al-Agha OM, Zhao Y, Tse K, Zeng T, Senz J, McConechy MK, Anglesio MS, Kalloger SE, *et al*: ARID1A mutations in endometriosis-associated ovarian carcinomas. *N Engl J Med* 363: 1532-1543, 2010.

12. Ramos P, Karnezis AN, Craig DW, Sekulic A, Russell ML, Hendricks WPD, Corneveaux JJ, Barrett MT, Shumansky K, Yang Y, *et al*: Small cell carcinoma of the ovary, hypercalcemic type, displays frequent inactivating germline and somatic mutations in SMARCA4. *Nat Genet* 46: 427-429, 2014.
13. Oyama Y, Shigeta S, Tokunaga H, Tsuji K, Ishibashi M, Shibuya Y, Shimada M, Yasuda J and Yaegashi N: CHD4 regulates platinum sensitivity through MDR1 expression in ovarian cancer: A potential role of CHD4 inhibition as a combination therapy with platinum agents. *PLoS One* 16: e0251079, 2021.
14. Cerami E, Gao J, Dogrusoz U, Gross BE, Sumer SO, Aksoy BA, Jacobsen A, Byrne CJ, Heuer ML, Larsson E, *et al*: The cBio cancer genomics portal: An open platform for exploring multi-dimensional cancer genomics data. *Cancer Discov* 2: 401-404, 2012.
15. Gao J, Aksoy BA, Dogrusoz U, Dresdner G, Gross B, Sumer SO, Sun Y, Jacobsen A, Sinha R, Larsson E, *et al*: Integrative analysis of complex cancer genomics and clinical profiles using the cBioPortal. *Sci Signal* 6: p11, 2013.
16. Cree IA, White VA, Indave BI and Lokuhetty D: Revising the WHO classification: Female genital tract tumours. *Histopathology* 76: 151-156, 2020.
17. Prat J and Oncology FCoG: FIGO's staging classification for cancer of the ovary, fallopian tube, and peritoneum: Abridged republication. *J Gynecol Oncol* 26: 87-89, 2015.
18. Livak KJ and Schmittgen TD: Analysis of relative gene expression data using real-time quantitative PCR and the 2(-Delta Delta C(T)) method. *Methods* 25: 402-408, 2001.
19. Clapier CR, Iwasa J, Cairns BR and Peterson CL: Mechanisms of action and regulation of ATP-dependent chromatin-remodelling complexes. *Nat Rev Mol Cell Biol* 18: 407-422, 2017.
20. He S, Wu Z, Tian Y, Yu Z, Yu J, Wang X, Li J, Liu B and Xu Y: Structure of nucleosome-bound human BAF complex. *Science* 367: 875-881, 2020.
21. Wade SL, Langer LF, Ward JM and Archer TK: MiRNA-mediated regulation of the SWI/SNF chromatin remodeling complex controls pluripotency and endodermal differentiation in human ESCs. *Stem Cells* 33: 2925-2935, 2015.
22. Ramirez J and Hagman J: The Mi-2/NuRD complex: A critical epigenetic regulator of hematopoietic development, differentiation and cancer. *Epigenetics* 4: 532-536, 2009.
23. Zhang J, Shih DJH and Lin SY: The tale of CHD4 in DNA damage response and chemotherapeutic response. *J Cancer Res Cell Ther* 3: 052, 2019.
24. Chen PM, Wong CN, Wong CN and Chu PY: Actin-like Protein 6A expression correlates with cancer stem cell-like features and poor prognosis in ovarian cancer. *Int J Mol Sci* 24: 2016, 2023.
25. Ji J, Xu R, Zhang X, Han M, Xu Y, Wei Y, Ding K, Wang S, Huang B, Chen A, *et al*: Actin like-6A promotes glioma progression through stabilization of transcriptional regulators YAP/TAZ. *Cell Death Dis* 9: 517, 2018.
26. Saladi SV, Ross K, Karaayvaz M, Tata PR, Mou H, Rajagopal J, Ramaswamy S and Ellisen LW: ACTL6A is co-amplified with p63 in squamous cell carcinoma to drive YAP activation, regenerative proliferation, and poor prognosis. *Cancer Cell* 31: 35-49, 2017.
27. Sun W, Wang W, Lei J, Li H and Wu Y: Actin-like protein 6A is a novel prognostic indicator promoting invasion and metastasis in osteosarcoma. *Oncol Rep* 37: 2405-2417, 2017.
28. Xiao S, Chang RM, Yang MY, Lei X, Liu X, Gao WB, Xiao JL and Yang LY: Actin-like 6A predicts poor prognosis of hepatocellular carcinoma and promotes metastasis and epithelial-mesenchymal transition. *Hepatology* 63: 1256-1271, 2016.
29. Zeng Z, Yang H and Xiao S: ACTL6A expression promotes invasion, metastasis and epithelial mesenchymal transition of colon cancer. *BMC Cancer* 18: 1020, 2018.
30. Xiao Y, Lin FT and Lin WC: ACTL6A promotes repair of cisplatin-induced DNA damage, a new mechanism of platinum resistance in cancer. *Proc Natl Acad Sci USA* 118: e2015808118, 2021.
31. Buccitelli C and Selbach M: mRNAs, proteins and the emerging principles of gene expression control. *Nat Rev Genet* 21: 630-644, 2020.
32. Yamamoto T, Kohashi K, Yamada Y, Kawata J, Sakihama K, Matsuda R, Koga Y, Aishima S, Nakamura M and Oda Y: Relationship between cellular morphology and abnormality of SWI/SNF complex subunits in pancreatic undifferentiated carcinoma. *J Cancer Res Clin Oncol* 148: 2945-2957, 2022.
33. Li C, Wang T, Gu J, Qi S, Li J, Chen L, Wu H, Shi L, Song C and Li H: SMARCC2 mediates the regulation of DKK1 by the transcription factor EGR1 through chromatin remodeling to reduce the proliferative capacity of glioblastoma. *Cell Death Dis* 13: 990, 2022.
34. Havranek O, Westin JR, Zhang M, Rawal S, Kwak LW, Neelapu SS and Davis RE: Integrated analysis of genomic and gene expression profiles in follicular lymphoma reveals subsets and driver genes of potential microenvironmental importance. *Blood* 122: 2487-2490, 2013.
35. Hu B, Lin JZ, Yang XB and Sang XT: The roles of mutated SWI/SNF complexes in the initiation and development of hepatocellular carcinoma and its regulatory effect on the immune system: A review. *Cell Prolif* 53: e12791, 2020.
36. Raab JR, Runge JS, Spear CC and Magnuson T: Co-regulation of transcription by BRG1 and BRM, two mutually exclusive SWI/SNF ATPase subunits. *Epigenetics Chromatin* 10: 62, 2017.
37. Marquez SB, Thompson KW, Lu L and Reisman D: Beyond mutations: Additional mechanisms and implications of SWI/SNF complex inactivation. *Front Oncol* 4: 372, 2014.
38. Wilson BG, Helming KC, Wang X, Kim Y, Vazquez F, Jagani Z, Hahn WC and Roberts CWM: Residual complexes containing SMARCA2 (BRM) underlie the oncogenic drive of SMARCA4 (BRG1) mutation. *Mol Cell Biol* 34: 1136-1144, 2014.
39. Yang T, Wang D, Tian G, Sun L, Yang M, Yin X, Xiao J, Sheng Y, Zhu D, He H and Zhou Y: Chromatin remodeling complexes regulate genome architecture in Arabidopsis. *Plant Cell* 34: 2638-2651, 2022.
40. Bowtell DD, Böhm S, Ahmed AA, Aspuria PJ, Bast RC Jr, Beral V, Berek JS, Birrer MJ, Blagden S, Bookman MA, *et al*: Rethinking ovarian cancer II: Reducing mortality from high-grade serous ovarian cancer. *Nat Rev Cancer* 15: 668-679, 2015.
41. Zhang FL and Li DQ: Targeting chromatin-remodeling factors in cancer cells: Promising molecules in cancer therapy. *Int J Mol Sci* 23, 2022.
42. Wang J, Zhong F, Li J, Yue H, Li W and Lu X: The epigenetic factor CHD4 contributes to metastasis by regulating the EZH2/ β -catenin axis and acts as a therapeutic target in ovarian cancer. *J Transl Med* 21: 38, 2023.